Electronic Supplementary Material (ESI) for Journal of Materials Chemistry A.
This journal is © The Royal Society of Chemistry 2023

Synergistic effects of Fe-substitutional-doping and surface close-contact Fe_2O_3/CeO_2 heterojunction in Fe/CeO_2 for enhanced CH_4 photocatalytic conversion

Hailong Tang [a], Meiling Wang [a,], Yongqing Ma [a, b], Xiao Sun [c], Min Wang [d,]* and Ganhong Zheng [a]*

[a] *School of Materials Science and Engineering, Anhui University, Hefei, 230601, China*

[b] *Institute of Physical Science and Information Technology, Anhui University, Hefei 230601, China*

[c] *Hefei National Laboratory for Physical Sciences at the Microscale, Key Laboratory of Surface and Interface Chemistry and Energy Catalysis of Anhui Higher Education Institutes, School of Chemistry and Materials Science, University of Science and Technology of China, Hefei 230026, China.*

[d] *School of Physics and optoelectronics engineering, Anhui University, Hefei, 230601, China*

*To whom correspondence should be addressed.

Tel: (86) 13856996630, E-mail: mlw@ahu.edu.cn, ahwm@ahu.edu.cn

Key words: CeO_2, Fe-substitutional-doping, Fe_2O_3/CeO_2 heterojunction, photocatalysis, CH_4 conversion

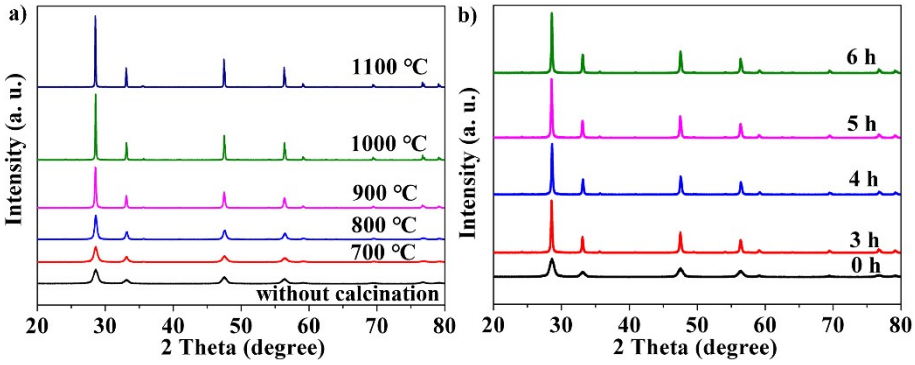

Fig. S1 XRD spectra of 1:3 Fe/CeO_2 calculated under varied a) temperature and b) time.

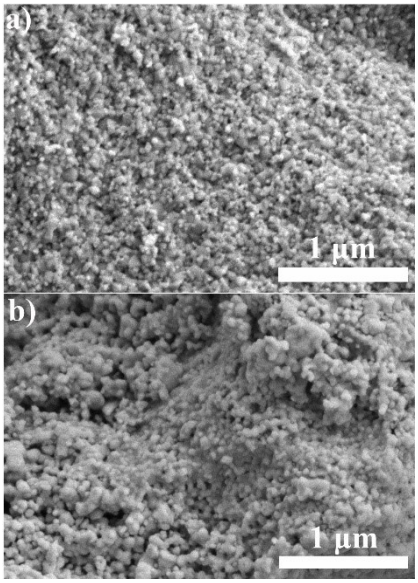

Fig. S2 a) SEM images of CeO_2-900/6 and b) 1:3 Fe/CeO_2-900/6 before picking.

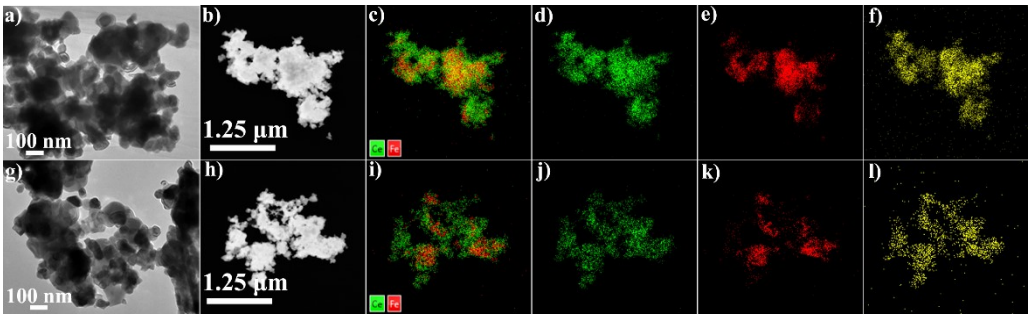

Fig. S3 TEM, STEM and EDS mapping images of 1:3 Fe/CeO_2-900/6 a-f) before and g-l) after pickling respectively.

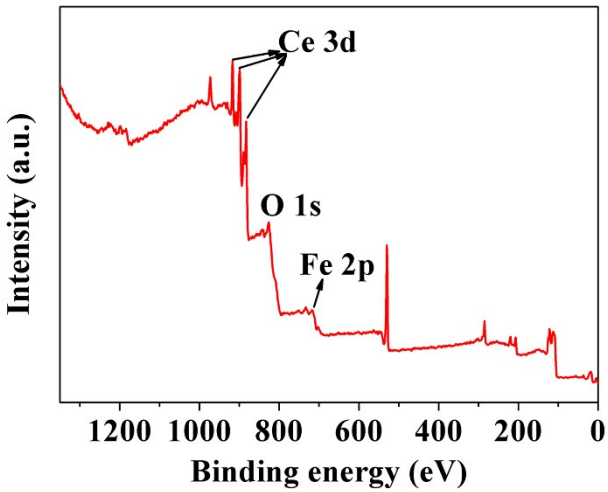

Fig.S4 XPS survey spectrum of 1:3 Fe/CeO_2-900/6.

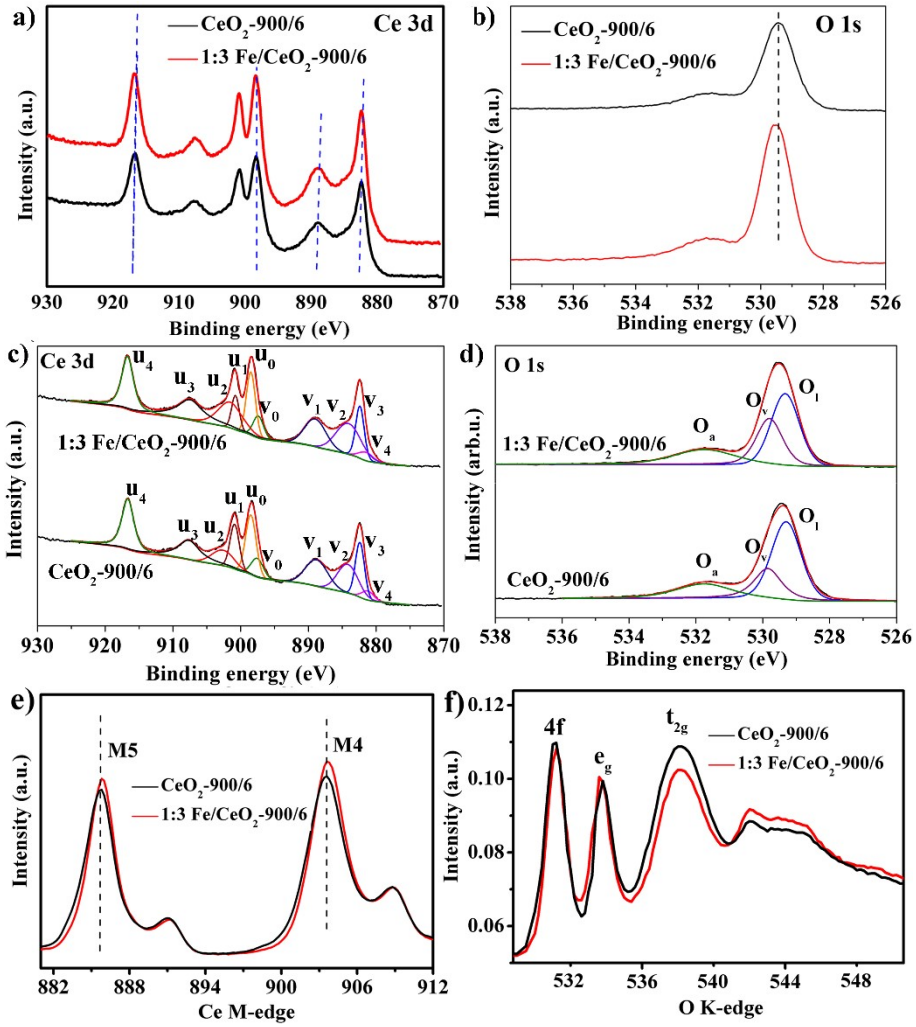

Fig. S5 a, b) High-resolution Ce 3d and O 1s XPS spectra of 1:3 Fe/CeO_2-900/6. c, d) Deconvoluted Ce 3d and O 1s XPS spectra of 1:3 Fe/CeO_2-900/6 and CeO_2-900/6 respectively. e, f) Ce M-edge and O K-edge XANES spectra of 1:3 Fe/CeO_2-900/6.

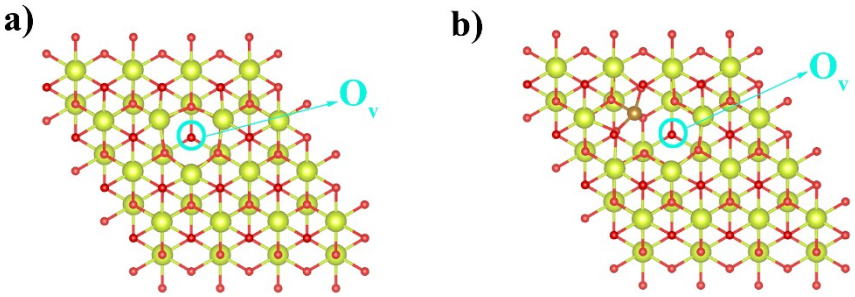

Fig. S6 Model structures of CeO_2 and Fe-substituted CeO_2 with O_v.

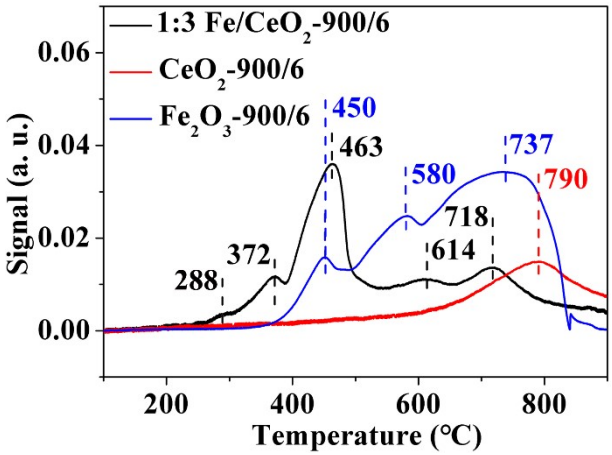

Fig. S7 H_2-TPR profiles of varied catalysts.

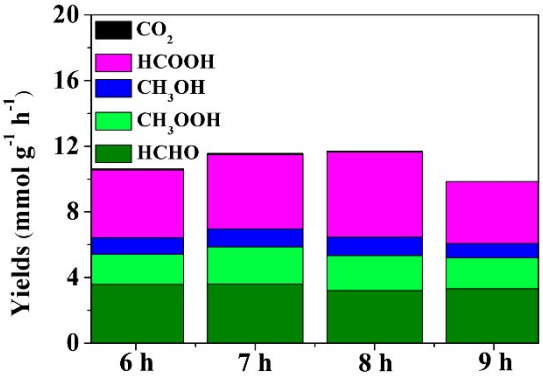

Fig. S8 Product yields over catalysts with prolonged calcination time.

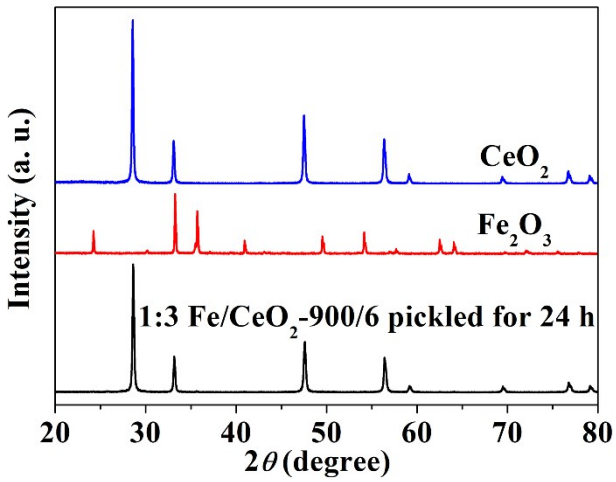

Fig. S9 XRD spectra of CeO_2, Fe_2O_3 and 1:3 Fe/CeO_2-900/6 pickled with pure hydrochloric acid solution for 24 h respectively.

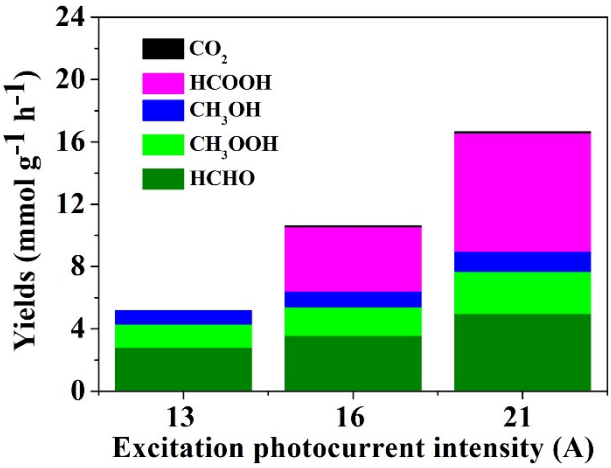

Fig. S10 Yields of C1 products using different light intensity.

Table S1 Products yields of 1:3 Fe/CeO_2-900/6 with HCl pickling time of 24 h.

Products	CH_3OH	HCHO	HCOOH	CH_3OOH	CO_2	Total
Yields (mmol $g_{cat.}^{-1}$ h^{-1})	0.66007	4.21538	0.74198	1.42045	0.01496	7.05284

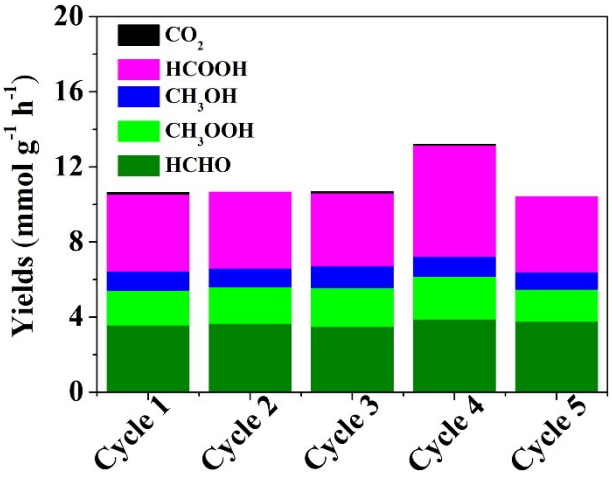

Fig. S11 Cycling tests of CH_4 conversion over 1:3 Fe/CeO_2-900/6.

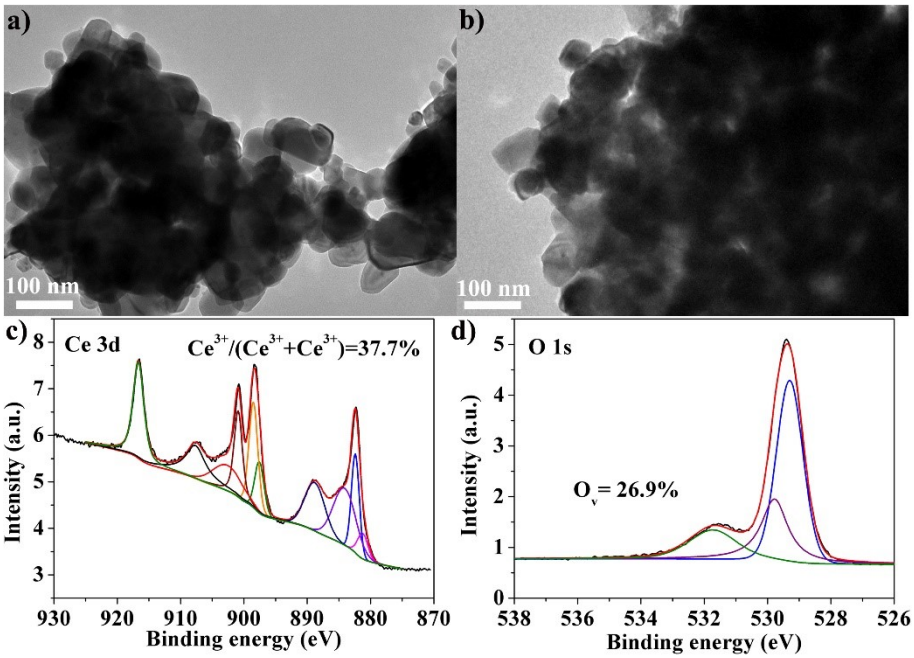

Fig. S12 a, b) TEM images of 1:3 Fe/CeO_2-900/6 before and after photocatalytic experiment, and c, d) deconvoluted high-resolution Ce 3d and O1s XPS spectra of 1:3 Fe/CeO_2-900/6 after illumination.

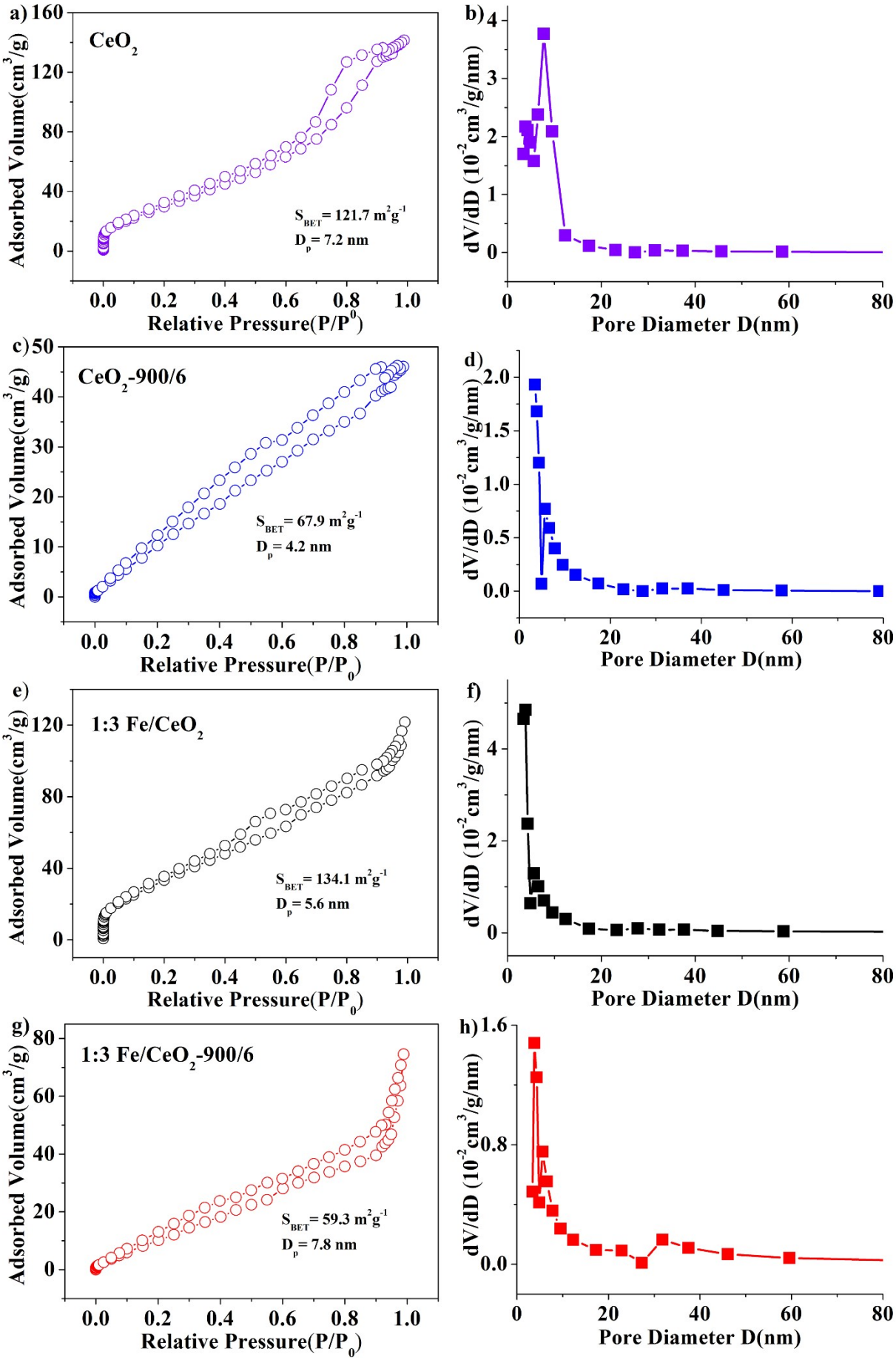
a)
CeO2
S_BET = 121.7 m2g-1
Dp = 7.2 nm
Adsorbed Volume(cm3/g)
Relative Pressure(P/P0)
b)
dV/dD (10-2cm3/g/nm)
Pore Diameter D(nm)
c)
CeO2-900/6
S_BET = 67.9 m2g-1
Dp = 4.2 nm
Adsorbed Volume(cm3/g)
Relative Pressure(P/P0)
d)
dV/dD (10-2cm3/g/nm)
Pore Diameter D(nm)
e)
1:3 Fe/CeO2
S_BET = 134.1 m2g-1
Dp = 5.6 nm
Adsorbed Volume(cm3/g)
Relative Pressure(P/P0)
f)
dV/dD (10-2cm3/g/nm)
Pore Diameter D(nm)
g)
1:3 Fe/CeO2-900/6
S_BET = 59.3 m2g-1
Dp = 7.8 nm
Adsorbed Volume(cm3/g)
Relative Pressure(P/P0)
h)
dV/dD (10-2cm3/g/nm)
Pore Diameter D(nm)

Fig. S13 The N_2 adsorption–desorption isotherms and corresponding pore size distribution curves for a, b) CeO_2, c, d) CeO_2-900/6, e, f) 1:3 Fe/CeO_2 and g, h) 1:3 Fe/CeO_2-900/6 respectively.

Table S2 Calculated Hirshfeld charge for the CeO_2 and * slabs respectively.

Models	Hirshfeld Charge		
	Ce	O	Fe
CeO_2	0.639	-0.349	/
*	0.637	-0.248	0.453

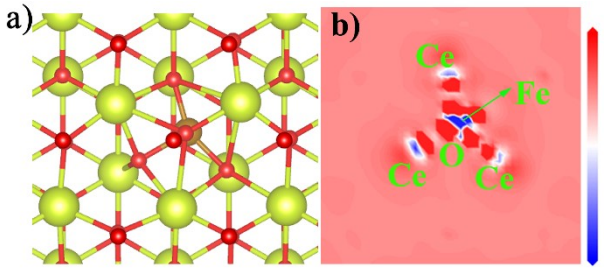

Fig. S14 a) Optimized structure and b) DCD maps of the Fe-interstitial-doped CeO_2 slab, plotted from -0.05 (blue) to 0.15 e $Å^{-3}$ (red).

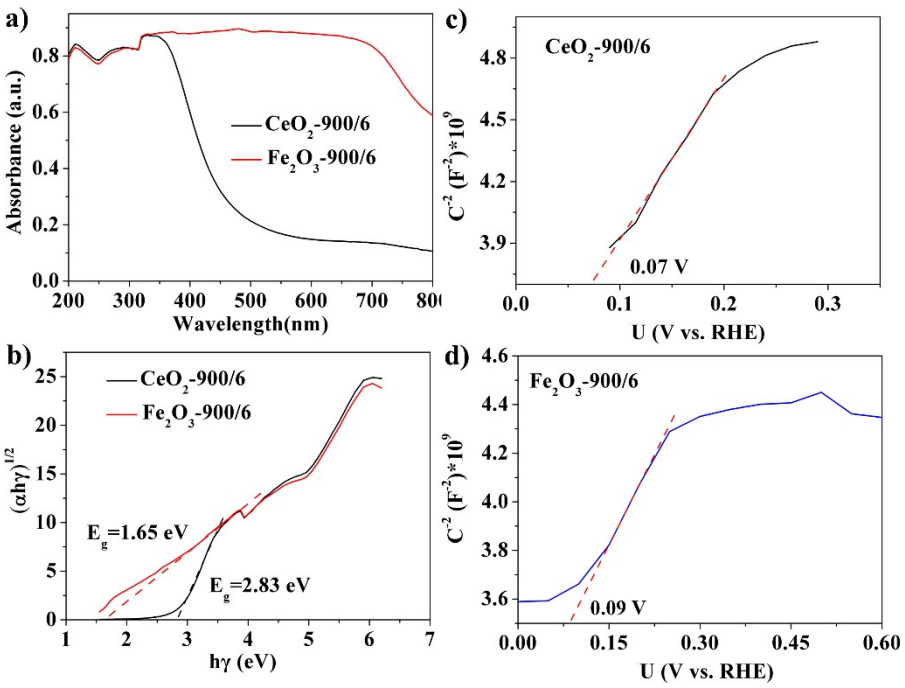

Fig. S15 a) UV-vis DRS spectra and b) bandgaps determined using $[Ah\gamma]^{1/2}$ vs hγ plots for varied CeO_2, c, d) Mott-Schottky plot of CeO_2-900/6 and Fe_2O_3-900/6 at the frequency of 1 kHz.

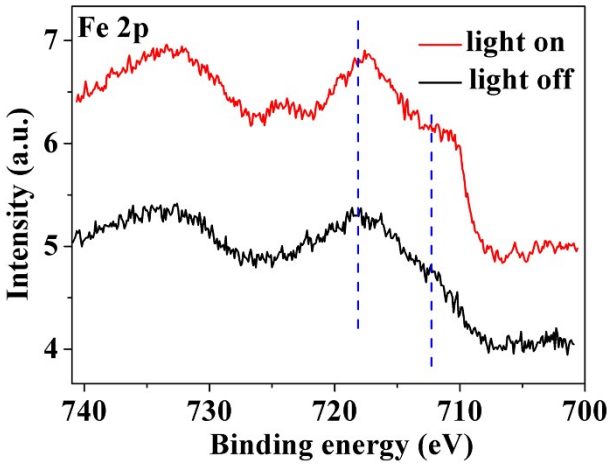

Fig. S16 High-resolution Fe 2p XPS spectra of 1:3 Fe/CeO_2-900/6 with and without illumination respectively.

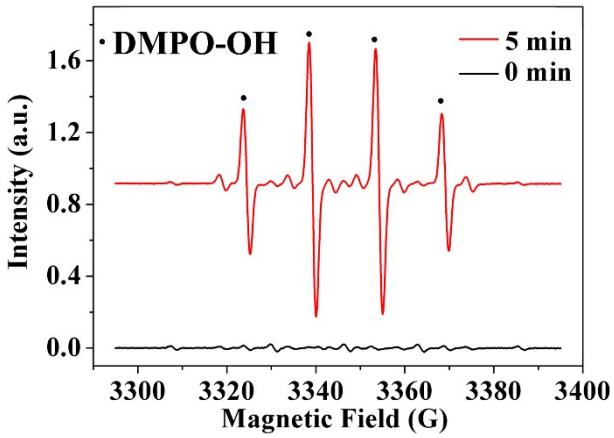

Fig. S17 ESR spectra of the reaction system.

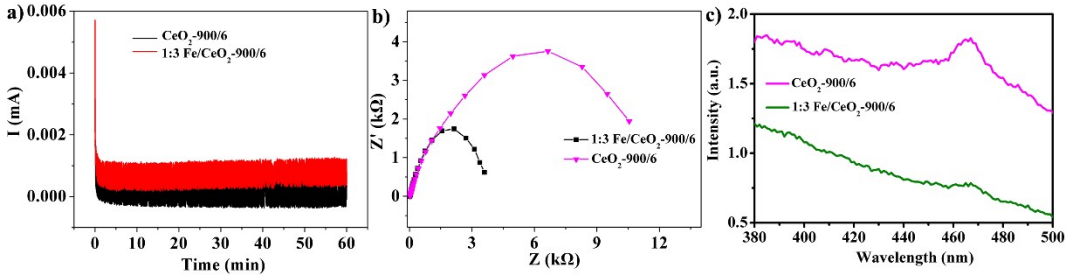

Fig. S18 a) The photocurrent curves, b) EIS spectra and c) PL spectra of 1:3 Fe/CeO_2-900/6 and CeO_2-900/6.

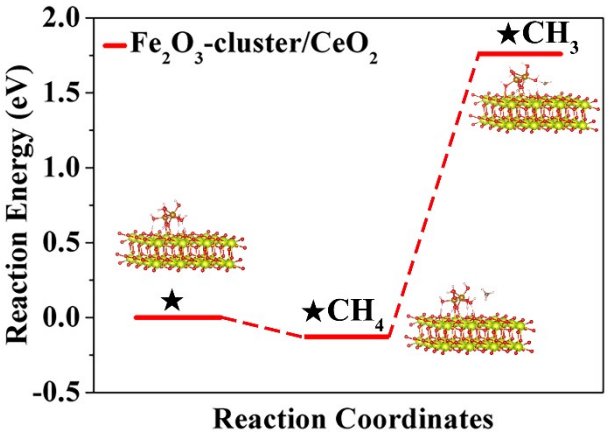

Fig. S19 DFT energy profile for CH_4 adsorption and activation to ❿CH_3 over Fe_2O_3-cluster/CeO_2 respectively.

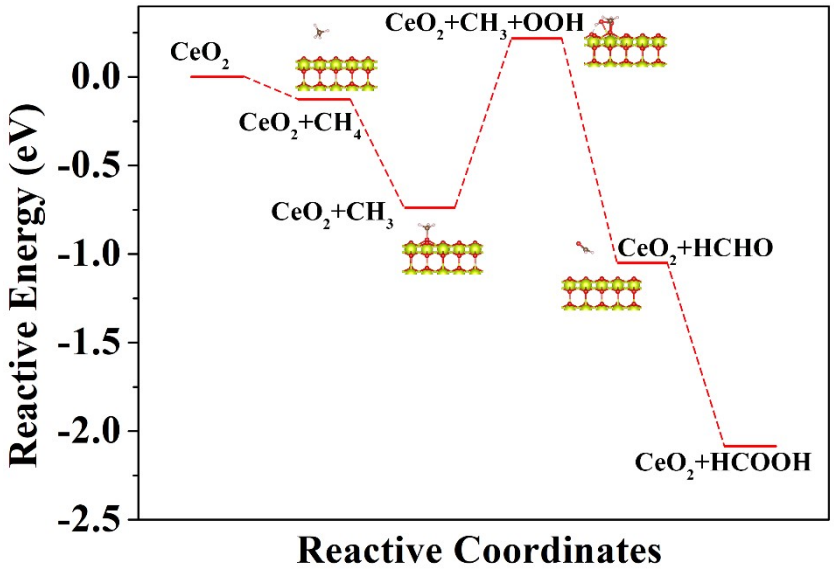

Fig. S20 Proposed reaction routes and DFT energy profiles for CH_4 photooxidation to C1 products over CeO_2.

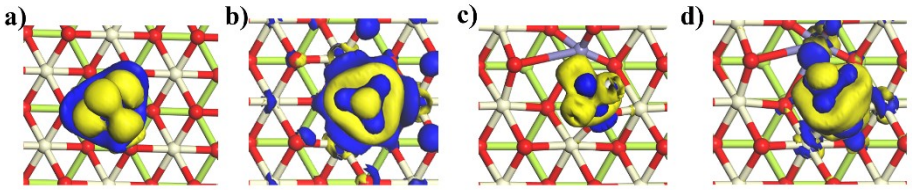

Fig. S21 DCD maps of CeO_2+CH_4, CeO_2+CH_3, *CH_4 and *CH_3 respectively. The isosurface value is 0.008 e $Å^{-3}$.

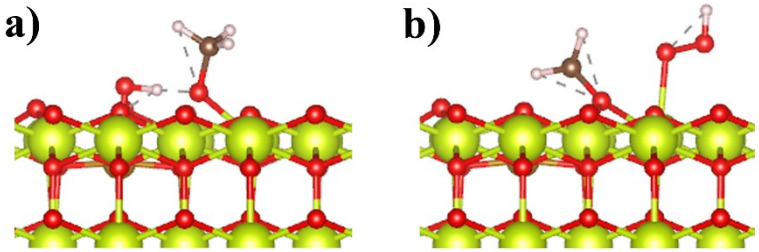

Fig. S22 Optimized structures of *CH_3+OH_{Fe} and *CH_3+OOH_{Ce} respectively.

Part S1 Details of the instruments and equipment used for catalysts characterization.

Morphologies and crystal structures of the catalysts were characterized using scanning

electron microscopy (SEM, S-4800, Hitachi, Japan), transmission electron microscopy (TEM, JEOL JEM-2100, Japan) and powder X-ray diffraction (XRD) spectra (Rigaku Industrial Corporation, Osaka, Japan). Fourier transform infrared (FTIR) spectra and UV–vis diffuse reflectance spectra (DRS) were recorded on the Vertex 80/Hyperion 2000 spectrometer (Bruker, Germany) and UV-vis absorption spectrometer (UV-vis DRS, U-4100, Shimadazu, Japan) respectively. Elemental surface chemical states and valence-band spectra were characterized using X-ray photoelectron spectroscopy (XPS, ESCALAB 250Xi, Thermo Scientific Inc., USA). H nuclear magnetic resonance (HNMR) spectra were measured on a JNM-ECZ400S NMR spectrometer (Japan). Specific surface areas and pore sizes were obtained via an the Quantachrome Instrument (USA). Electron paramagnetic resonance (EPR) spectra were measured on a EPR spectrometer (EMX plus 10/12, Bruker, Germany).

Part S2 DFT computational details.

All the density functional theory (DFT) calculations were carried out using the Dmol^3 code of Materials Studio 2019.[1] The exchange-correlation potential was calculated by the generalized gradient approximation (GGA) with the Perdew-Burke-Ernzerhof (PBE) functional.[1] The interactions between electronics and ions were described using the DFT semi-core pseudo potentials (DSPPs) core treatment, which replaces core electrons by a single effective potential and introduces some degree of relativistic correction into the core. The geometry optimization convergences tolerance was set to 0.002 Ha·Å^{-1} (1 Ha = 27.21 eV), and the total energy convergences was set to 10^{-6} Ha. The Brillouin zone was sampled with 2×2×1 Monkhorst-Pack k-point mesh, and a smearing of 0.005 Ha was applied to speed up electronic convergence. The 2-layer 2×2 supercell of CeO_2 (1 1 1) slab with 96 atoms (six atomic layers) was used to build the calculation models. Spin polarization was also applied to our calculations, and the real space cutoff radius was maintained as 5.0 Å.[2, 3] The Ce and O atoms in the bottom three layers were fixed, and the other atoms were fully relaxed. The thickness of the vacuum layer in multi-layer calculation models was set to 20 Å to avoid the unwanted interaction between the slab and its period images.

References

1 Y. Jiang, C. Lai, Q. Li, W. Gan, L. Yang, Z. Yang, R. Lin, X. Wang, X. Zhu, The poisoning effect of KCl and K_2O on CeO_2-TiO_2 catalyst for selective catalytic reduction of NO with NH_3, Fuel. 280 (2020) 118638.

2 X. Song, P. Ning, C. Wang, K. Li, L. Tang, X. Sun, Catalytic hydrolysis of COS over CeO_2 (110) surface: A density functional theory study, Appl. Surf. Sci. 414 (2017) 345-352.

3 H. Tang, T. Ju, Y. Dai, M. Wang, Y. Ma, M. Wang, G. Zheng, Ultrahigh efficiency CH_4 photocatalytic conversion to C1 liquid products over cheap and vacancy-rich CeO_2 at 30 ℃, J. Mater. Chem. A. 10 (2022) 18978-18988.